Lift Corrections to Transonic Equivalence Rule: Examples

H. K. Cheng*
University of Southern California, Los Angeles, Calif.

The lift correction to the transonic equivalence rule, with specific reference to its dependence on the wing planform and load distribution, is studied. Calculations of the equivalence-body cross-sectional area, $S_e(x)$, are performed for examples from three families of wing planforms; the results are applied to the analysis of a Mach .98 transport, considering alternative wing designs. An increase in $S_e(x)$ due to nonlinear lift effects is found to be significant: a rise in $S_e(x)$ by 35% above the zero-lift maximum occurs over a distance comparable to the root chord. However, in changing from a symmetrical to an asymmetrical wing arrangement, the maximum of the lift correction to $S_e(x)$ can be reduced by as much as a factor of four, with a nearly eight-fold reduction in the correction to the equivalent source strength, dS_e/dx.

I. Introduction

AT transonic speeds the flow disturbance extends laterally to a great distance from the body. The three-dimensional flow structure far from the body is an essential aspect which determines the drag rise, maneuverability, and other aircraft characteristics in the transonic range. The most important aerodynamic concept in this regard is, perhaps, the transonic equivalence rule, or the area rule, of Oswatitsch and Whitcomb.[1-3] This rule requires, however, a modification to account for the lift contribution which proves to be essential in the operating ranges of modern aircraft.[4,5] As a sequel to the works of Refs. 4 and 5, this paper will examine more specifically the extent to which the lift corrections depend on the planform and the mode of load distribution; supporting calculations for three types of lifting surface are studied.

It is well established from the classical linear theory that the flow far from a *slender* body (or low aspect-ratio wing) at small incidence may be identified with that produced by an (equivalent) axisymmetric body having the same (axial distribution of) cross-sectional area $S_c(x)$.[7] The contributions by Whitcomb,[1] Oswatitsch,[2] and other early workers on the transonic equivalence rule,[3,8] lie essentially in their demonstrations showing that the same rule applies also in the case with a *nonlinear* transonic outer flow. This transonic equivalence has been extended to wings with incidence comparable to the thickness,[9] and with aspect ratio as high as unit order.[10] Underlying Refs. 1-3 and 8-10 is the concept that the body affects the nonlinear transonic flow field far from it in the same manner as a *line source* with a strength proportional to dS_c/dx. Hayes[11] is, perhaps, among the first in recognizing the need for departing from this concept due to lift; in Hayes' linearized study, the lift effect on the outer flow appears as one of a line doublet. As brought out by Cheng[12] and Barnwell,[13] the line source and line doublet pair provides a fairly adequate representation of the body for the outer flow (without recourse to other singularities), even if lift were to dominate. The present study is based on the recent work of Cheng and Hafez,[4,5] which is more complete and correct in the sense of an asymptotic theory.

In a more recent work reported in Ref. 14, Barnwell gives results similar to those of Cheng and Hafez,[4,5] using body-oriented coordinates. Except for an error in Barnwell's analysis, which can be readily corrected,† his basic results do agree with those of Cheng and Hafez. An interesting aspect in Barnwell's recent study concerns the modeling of leading-edge separation. Its validity requires a critical examination and will not be discussed here.

The major content of this paper is concerned with the computed results that are to be discussed in Secs. IV and V. To indicate more clearly the scope and limitations of the theory, various theoretical requirements are stated in Sec. II, where several important parameters are defined. A summary of the theory of the equivalence rule involving lift is given in Sec. III with a discussion of its relevance to the drag rise study. In Sec. IV we discuss and perform calculations of the equivalent-body cross-sectional area, $S_e(x)$, and related quantities for three families of planform with various load distributions. These calculations are applied in Sec. V to the study of lift effect for a Mach 0.98 transonic transport with specifications similar to those in Refs. 15 and 16.

II. Assumptions and Basic Parameters

A. Assumptions and Geometrical Requirements

The theory[4,5] on which the subsequent study is based assumes a slightly perturbed steady inviscid flow with uniform freestream. The lift is carried mainly by a nearly planar wing, of which the thickness and lift distributions are prescribed. Only wing planforms permitting smooth distributions, such as those of the Concorde, the symmetric swept, and the oblique designs, will be considered. The theory assumes a smooth lift distribution which vanishes at both upstream and downstream ends of the planform. In practice this can be realized by proper wing twist, or more easily by *tip fairing* (rounding off the leading-edge portion of the planform contour near the tip, as for the Concorde).

The area of the cross section transverse to the wind axis, $S_c(x)$, is assumed given; it may also include that of the *slender* fuselage lying close to the wing plane. The wing camber geometry can be determined from the assumed lift distribution, using the linear transonic theory.[5,6] To avoid solution breakdown at the edges, the lift distribution is assumed to be bounded at both the trailing and leading edges.‡ In particular, the inverse square root type singularity is to be avoided. This point is amplified in Fig. 1 which illustrates a cross section with dropped leading edges. In passing, it may be noted that a small round leading edge with a radius comparable to the square of the thickness is also admissible to the theory, although the analysis cannot be used to treat the leading-edge region itself.

Received Dec. 9, 1975; revision received Oct. 22, 1976.
Index categories: Aircraft Aerodynamics (including Component Aerodynamics); Subsonic and Transonic Flow.

*Professor, Aerospace Engineering. Member AIAA.

†The error is traceable to Eq. (40) of Ref. 14 where a correction to the transferred tangency condition was omitted.

‡The theory presented in Refs. 4 and 5 assumes that the lift distribution vanishes at the edges, which is more conservative than the boundedness requirement stated in above.

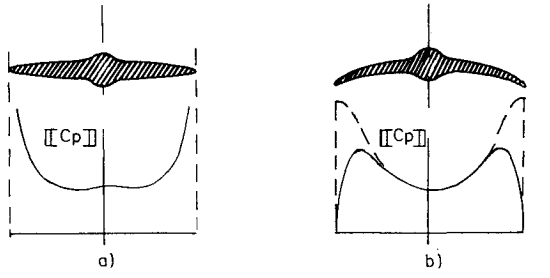

Fig. 1 Distributions of pressure jump a) with leading-edge singularities, and b) with the leading-edge singularities removed. The dotted curve refers to the case with a finite nonvanishing jump at the leading edge.

B. Coordinates—Thickness, Lift, and Other Parameters

A Cartesian coordinate system (x,y,z) is used, with the z-axis pointing in the lift direction. Alternately, cylindrical polar coordinates (x,r,ω) are also used, with r representing distance from the x-axis, and ω the azimuthal angle. Associated with x and r are two reference length scales l and b. Length l characterizes the axial distribution of the thickness or the lift (whichever predominates), and the length b is simply the half span.

Three parameters, λ, τ, and α, are used to define the wing geometry and the lift (of a given basic planform). Parameter λ is the ratio of the two lengths

$$\lambda \equiv b/l \tag{1}$$

and may be taken to indicate an average sweep angle of the leading edges. Parameters τ and α are defined in terms of the maximum cross-sectional area $S_{c\,\max}$ and the total lift, respectively:

$$\tau \equiv S_{c\,\max}/bl \qquad \alpha \equiv (\text{Lift})/\rho_\infty U^2 b^2 \tag{2}$$

Obviously, α and τ are the generalized camber and thickness ratio suggested by linear transonic (slender-body) theory; they are both required to be small.

C. Four Reduced Parameters—Nonlinear Lift Effects

A complete specification of the system at hand requires at least four parameters (e.g., τ,α,λ, and the Mach number M_∞). The set of four parameters which appear in the final formulation of the reduced problem for the nonlinear outer flow is (adopting the notations of Refs. 4 and 5)

$$\left.\begin{aligned} &\epsilon = [(\gamma+1)M_\infty^2 \tau\lambda]^{1/2} \qquad \sigma_\cdot \equiv [(\gamma+1)M_\infty^2 |\ell n\epsilon|\lambda^3]^{1/2}\alpha\tau^{-1/2} \\ &\Gamma_\cdot \equiv \delta(\gamma+1)^{-1}|\ell n\epsilon|^{-1}\lambda^{-2} \qquad K \equiv (M_\infty^2-1)\lambda^2\epsilon^{-2} \end{aligned}\right\} \tag{3}$$

where γ is the gas specific-heat ratio. Each of these parameters is associated with a particular effect or feature of the nonlinear outer problem. Except for an unbounded $\sigma_\cdot$, the parameter ϵ is the ratio of the transverse length scale of the inner flow region, b, to that of the outer region far from the wing. The choice of the parameter set Eq. (3) permitted Cheng and Hafez[4,5] to deduce an equivalence rule by considering (a single limit) $\epsilon \to 0$, while keeping $\sigma_\cdot$, $\Gamma_\cdot$, and K fixed. In the limit $\epsilon \to 0$, the outer flow sees the body and its vicinity as a line segment along the x-axis, and the presence of the wing and body is felt mainly in the form of a *line source* and *line doublet*. The latters are controlled mainly by $\sigma_\cdot$ and $\Gamma_\cdot$.

For an unbounded $\sigma_\cdot$, corresponding to a vanishing thickness ratio, the transverse length ratio ϵ in Eq. (3) may be replaced by other products of α and λ, independent of the thickness ratio τ, with the corresponding changes in the definitions for $\sigma_\cdot$, $\Gamma_\cdot$, and K. However, the two systems are equivalent and the consideration of the other parameter set is unnecessary for the present purpose.[4,5]

It is of interest to point out the reason why the relatively weak nonlinear corrections (due to lift) to the Jones solution[6] should produce effects of first-order importance in the outer flow. The differential equation governing the inner equation may be written as

$$\phi_{yy}+\phi_{zz} = (M_\infty^2-1)\phi_{xx}$$
$$+M_\infty^2 U^{-1}\frac{\partial}{\partial x}\left[\left(1+\frac{\gamma-1}{2}M_\infty^2\right)\phi_x^2+\phi_y^2+\phi_z^2\right] \tag{4}$$

where ϕ is the perturbation velocity pontential. The three terms inside the square bracket on the right represent the *second-order compressibility corrections* to the velocity divergence, and may be interpreted as a distribution source in the cross-flow plane near the wing. Far enough from the axis $(r \gg b)$, the integrable part of this distributed source should produce an effect equivalent to a line source. This line source does not vanish with the thickness, because ϕ_x^2, ϕ_y^2, and ϕ_z^2 lack the skew symmetry with respect to z. With high enough lift, the source strength generated in this way can be comparable to, or even greater than, the rate produced by the actual geometrical cross-section area $S_c(x)$. The ratio of these two source strengths must clearly be proportional to α^2/τ which is identifiable with $\sigma_\cdot^2$. §

The terms ϕ_y^2 and ϕ_z^2 signify (twice) the kinetic energy of the cross flow and are absent from the classical transonic small-disturbance equation. The line source contributed by these two terms gives rise to a nonvanishing total volume flux, hence, an equivalent afterbody.

III. Summary of the Reduced Problem: The Equivalence Rule

A. Reduced Nonlinear Problem

Like the classical equivalence rule,[1-3,7-9] Cheng and Hafez's theory[4,5] stipulates an inner region around the wing (or the aircraft) and an outer region far from the wing. The inner flowfield is described basically by the linear transonic solution, with nonlinear and other higher-order corrections. This solution breaks down at a distance of the order b/ϵ from the axis, where the problem is reformulated with reduced variables:

$$\tilde{x} = x/l \quad \eta = \epsilon r/b \quad \omega \text{ and } \tilde{\phi} = \phi/\tau v b \tag{5}$$

where the transverse coordinate has been rescaled. The differential equation (to the leading order) governing this outer region is none other than the familiar transonic small-disturbance equation[9,11]

$$-\left(K\tilde{\phi}_{\tilde{x}}+\frac{1}{2}\tilde{\phi}_{\tilde{x}}^2\right)_{\tilde{x}}+\eta^{-1}(\eta\tilde{\phi}_\eta)_\eta+\eta^{-2}\tilde{\phi}_{\omega\omega}=0 \tag{6}$$

with

$$K = (M_\infty^2-1)/(\gamma+1)M_\infty^2\tau\lambda$$

consistent with Eq. (3). In the outer variables $(\tilde{x}, \eta, \omega)$, the inner region shrinks to the vicinity of the axis [$\eta = 0(\epsilon)$, to be sure] where Eq. (6) admits a development, with $\sigma_1 = \sigma_\cdot |\ell n\epsilon|^{-1/2}$

$$\tilde{\phi} \sim (2\pi)^{-1}S_e'(\tilde{x})\cdot\ell n\eta+(2\pi)^{-1}\sigma_1 F(\tilde{x})\eta^{-1}\sin\omega+\beta_o(x)$$
$$+\ldots+(8\pi)^{-2}\sigma_1^2\frac{\mathrm{d}}{\mathrm{d}x}(F_{\tilde{x}})^2\cdot[2(\ell n\eta)^2+\cos 2\omega]+\ldots. \tag{7}$$

§Note that $\sigma_\cdot^2 \propto |\ell n\epsilon|\alpha^2\tau^{-1}$ where the factor $\ell n\epsilon$ results from the matching detail of the inner and outer solutions.[4,5]

where the first term signifies a line source and the second a line doublet. Matching this with the inner solution identifies the doublet strength with the lift, and S_e' with a source strength (expressible in terms of $(d/dx)S_e$ and the nonlinear lift effects described in the preceeding section).[5] The function $F(\bar{x})$ is simply the lift at $\bar{x}$ normalized by its value at $\bar{x}=1$. The expression of $S_e'(\bar{x})$ will be more closely delineated later in Sec. IIIB. The function $\beta_o(x)$ signifies a feedback from the nonlinear outer flow, and is a part of the unknowns of the boundary-value problem. The last term involving the derivative of $F_{\bar{x}}^2$ is fixed once the lift distribution $F(\bar{x})$ is given.

Finally, the far-field condition is (excluding the positive x-axis)

$$\tilde{\phi}\to 0 \qquad \text{as} \qquad \bar{x}^2+\eta^2\to\infty \tag{8}$$

Equations (6-8) complete the specification of the boundary value problem of the outer flow.

B. Equivalence Rule

The above formulation shows that the strength of the line source and the line doublet are the only two functions of $\bar{x}$ through which the wing geometry and lift distributions can influence the outer flow. Therefore, the structure of the outer nonlinear flow at a specified transonic parameter K, including the shock and sonic boundaries, is the same, as long as the distributions $S_e'(\bar{x})$ and $\sigma_1 F(\bar{x})$ remain unchanged. In applying the rule, the correlation must, of course, be carried out in the reduced outer variables of Eq. (5). Since $c_p=-2\tau\lambda\tilde{\phi}_{\bar{x}}$, the ratios $c_p/\tau\lambda$ and $(M^2-1)/\epsilon^2$ will be correlated as functions of $\bar{x}$, η, and ω; sonic and shock boundaries may be correlated in the form of $\bar{x}=g(\eta,\omega;K)$. The drag rise due to shock loss in the outer flow, D_w, can be correlated as

$$D_w/\rho_\infty U^2 b^2\tau^2 M_\infty^2 = f(K) \tag{9}$$

The function $f(K)$ is of *unit* order for a fully developed shock in the outer region.

C. Form of S_e'

The line-source can be expressed as a sum consisting of the geometrical cross-sectional area $S_c(x)$ and terms that are dependent nonlinearly on the lift,[5]

$$S_c'(\bar{x}) = \frac{d}{dx}\{S_c(x)+\sigma_\cdot^2[(8\pi)^{-1}(1+(2|\ell n\epsilon|)^{-1})F_{\bar{x}}^2 + (2|\ell n\epsilon|]^{-1}\tilde{T}(\bar{x})+8^{-1}\sigma_\cdot^2\Gamma_\cdot\tilde{E}(\bar{x})\} \tag{10}$$

with

$$\tilde{E}(\bar{x}) = \frac{1}{4\pi}\int_{-\infty}^{\infty}\int_{-\infty}^{\infty}[\![\varphi(\bar{x},y)]\!]_y\cdot[\![\varphi(\bar{x},y_1)]\!]_{y_1}\cdot\ell n\left|\frac{1}{y_1-y}\right|\,dy\,dy_1$$

$$\tilde{T}(\bar{x}) = \frac{1}{4\pi}\int_{-\infty}^{\infty}\int_{-\infty}^{\infty}[\![\varphi(\bar{x},y)]\!]_{\bar{x}}[\![\varphi(\bar{x},y_1)]\!]_{\bar{x}}\cdot\ell n\left|\frac{1}{y_1-y}\right|\,dy\,dy_1$$

where $[\![\varphi]\!]$ is the potential jump normalized by $\alpha Ub,y$ and y_1 by b; subscripts x, y, and y_1 refer to partial derivatives. In view of the total derivative on the right of Eq. (10), the quantity inside the curley bracket may be duly referred to as the *cross-sectional area* of the *equivalent body* dS_e/dx. To be sure, $F(\bar{x})$ is a dimensionless lift at $\bar{x}$, related to $[\![\varphi]\!]$ as

$$F(\bar{x}) = \int_{-\infty}^{\infty}[\![\varphi]\!]\,dy \quad \text{and} \quad F(1)=1 \tag{11}$$

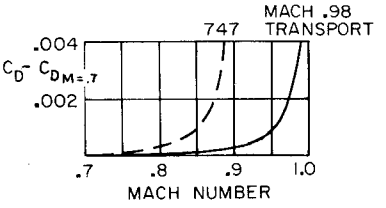

Fig. 2 Increase of drag coefficient near Mach one (Goodmanson 1971).

$S_c(x)$ and $S_e(x)$ have been normalized by the maximum geometrical cross-sectional area.

The form of the function $\tilde{E}(\bar{x})$ associated with $\sigma_\cdot^2\Gamma_\cdot$ is recognizable as a normalized kinetic energy in the Trefftz plane (i.e., the vortex drag). Interestingly, $\tilde{T}(\bar{x})$ assumes a form identical to that of $\tilde{E}(\bar{x})$, with the differential pressure replacing the differential side wash. It can be shown on the basis of Eq. (10) that $\tilde{T}(\bar{x})$ is nonnegative, as is $\tilde{E}(\bar{x})$. Therefore Eq. (10) implies to an inequality

$$S_e(x)\geq S_c(x) \tag{12}$$

D. Equivalence Rule and Transonic Drag Rise

The source and doublet distributions may be used as a *smoothness* and *slenderness* guide in transonic transport design in a manner analogous to the application of the classical area rule.[15,16] It is noted that most modern designs use high-aspect-ratio swept wings, employing "supercritical airfoils."[17-19] Implicit in the present study, as well as in the area-rule studies of Refs. 15 and 16, is the assumption that the component flow around the wing can be made "shock-free' under the cruise condition.¶ The shock loss in the outer flow should then be responsible for the transonic drag rise.

The drag rise characteristics of a transonic transport design has been compared with that of the Boeing 747 by Goodmanson[15] (Fig. 2). A transonic drag increase of $\Delta C_D=0.002$ is commonly used to define a "drag rise Mach number," and this value represents an appreciable and consequential drag increment. On the other hand, from Eq. (9) one has the drag coefficient associated with shock loss in the outer flow

$$C_{D_W} \equiv (\text{drag rise})/\tfrac{1}{2}\rho_\infty U^2(\text{wing area}) = \tfrac{1}{2}\tau^2 M_\infty^2 \mathcal{A}R f(K) \tag{13}$$

where f is a function of K only for a given pair of $S_e(x)$ and $\sigma_1 F(x)$, but is generally of *unit* order except at large $\sigma_\cdot$. [For $\sigma_\cdot\gg 1$, $f=0(\sigma_\cdot^2)$]. Therefore, C_{DW} in the transonic equivalence rule is generally gauged by $\tau^2 M_\infty^2 \mathcal{A}R/2$. If we take the Goodmanson design[15] as an example, one has $M_\infty=0.98$, $\mathcal{A}R=6.8$, $\tau=0.0263$, and thus $C_{D_W}\simeq(0.00226)f(K)$. This indicates that a drag rise of the order 0.002 indeed may be accounted for by the outer-flow shock loss and therefore is controllable through application of the equivalence rule.

IV. Calculating $F_{\bar{x}}^2$, $\tilde{E}$, and $\tilde{T}$

With ϵ, $\Gamma_\cdot$, and $\sigma_\cdot$ determined from the design specification, the axial distributions S_e and F controlling the outer flow will depend on the distributions of $[\![\varphi_x]\!]$ and $[\![\varphi_y]\!]$ through $F_{\bar{x}}^2$, $\tilde{E}$, and $\tilde{T}$ (cf. Eq. (10)).** The latter three functions are generally of unit order, provided the length scales b and l are properly chosen. However, their magnitudes and gradients may differ, depending on the type of wing

¶If the supercritical component flow around the high aspect-ratio wing is not shock free, the resulting drag rise would be many times that considered here.

**The distribution $F_{\bar{x}}^2$ also represents the nonlinear part of the inner boundary condition at the axis [cf. Eq. (7)]. The square root of it yields, of course, the derivative of the doublet strength.

planform, and, to a lesser degree, on the chordwise and spanwise lift distribution over a given planform. The following will present and compare F_x^2, $\bar{E}$, and $\bar{T}$ for specific planforms and lift distributions of interest. Throughout this section, the tildes over $\bar{x}$, $\bar{T}$, and $\bar{E}$ will be dropped for convenience.

A. Three Families of Planar Wings

Among the planforms commonly considered for high-speed designs, there are three families (main types), to which the equivalence rule is applicable: the Concorde (delta), the symmetric swept, and the oblique (asymmetric swept). The first type of planform may, of course, be regarded as a special case of the (now conventional) symmetric swept wings. The distinction is, however, mainained here to differentiate the symmetric swept wings of moderate and high aspect ratios from those comparable to the Concorde wing. Characterizing the dimensions of these planforms are the distances, measured from tip to tip, along the flight and transverse directions, referred to respectively as the overall wing chord c_o and the half-span b. (For wing alone, there is no distinction between c_o and l.)

The morphology in the present study will be confined mainly to these three wing families. The results obtained for $E(x)$ and $T(x)$ in this section are independent of the parameters $\sigma_\cdot$ and ϵ as well as the physical reference quantities $S^*_{\max}$ and l. The results should, therefore, be useful for computing the equivalent cross-sectional area for design analyses. In application to a complete configuration, the body is taken to be l in most cases (unless $\sigma_\cdot$ is excessively large). If we assume that no additional lift is caused by the body, the present calculation may then be used for the study of a complete configuration through proper variable transformations (cf. Sec. VA).

B. Calculation of F^2, $E(x)$, and $T(x)$

Except in cases with a uniform load, the distribution of $[\![\varphi_x]\!]$ corresponding to the pressure jump is assumed to vanish at the leading and trailing edge with a square-root singularity (in accordance with the smooth entry requirement of Sec. IIA). The spanwise circulation distribution in the form of $[\![\varphi]\!]_{T.E}$ is assumed to be elliptic, or as close to being elliptic as possible, inasmuch as the inviscid drag is given by the vortex drag in a truly shock-free flow.††

Concorde

The specific planform of this type, for which computations are made, is one with a leading-edge contour $y=a(x)$ shown in Fig. 3a. When the leading-edge sweep parameter $\lambda \equiv b/l$—i.e., b/c_0—is specialized to 1/(2.4), the leading-edge contour closely reproduces that of the Concorde. We assume that the lift distribution vanishes smoothly at, and downstream of, the (straight) line $x=1$ (cf. the dotted line in Fig. 3a). A distribution of the perturbation potential jump is assumed for this case (for $|y|<a(x)$) as

$$[\![\varphi]\!] = A(x)a^3(x)\cdot(1-\zeta^2)^{3/2}\cdot P(\zeta^2) \qquad (14)$$

where $\zeta \equiv y/a(x)$ and $P(\zeta^2)$ is polynominal in ζ^2 with coefficients being suitable functions of x. The resulting distributions of F_x^2, $T(x)$, and $E(x)$, under Eq. (14), turn out to be far less sensitive to the mode of $[\![\varphi]\!]$ than to the planform assumed. Typical distributions of $[\![\varphi]\!]$, $[\![\varphi_x]\!]$, and $[\![\varphi_y]\!]$ generated from an 8-deg (four-term) polynomial are shown in Fig. 4. The resulting axial lift distribution $F(x)$ turns out to be very close to the *square* of the local half span $a(x)$, hence, comparable to a flat-plate wing of the same planform. Thus, the distribution of $[\![\varphi]\!]$ assumed may be regarded as being reasonable. The resulting distributions of

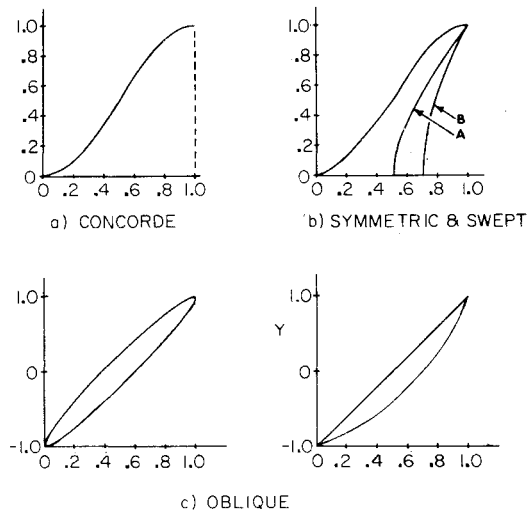

Fig. 3 Particular planforms studied.

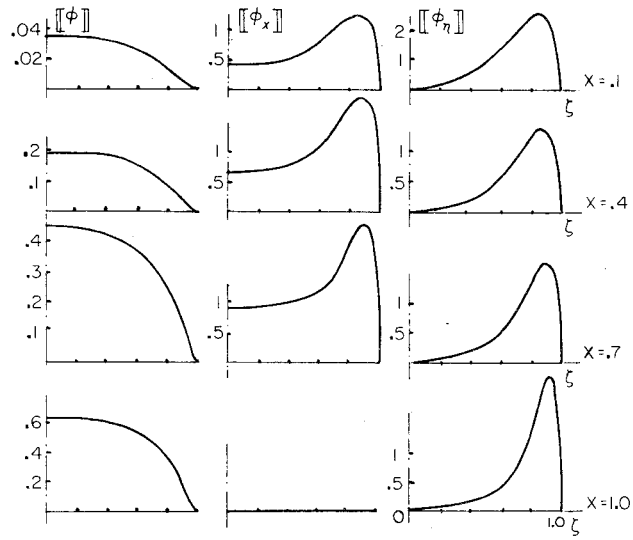

Fig. 4 Spanwise distributions of lift and vorticity jumps at different x-stations corresponding to eight-degree polynomial in Eq. (14).

F_x^2, T, and E (computed from explicit forms) are plotted as dash-dot curves in Figs. 5a, 5b, and 5c.

It is observed that the minimum value of the dimensionless kinetic energy $E(x)$ for a prescribed (local) lift $F(x)$ is

$$E_{\min}(x) = \left(\frac{1}{2\pi}\right)\left(\frac{F}{a}\right)^2 \qquad (15)$$

which becomes $1/2\pi$ at $x=1$. The value of $E(1)$ given by the dash-dot curve in Fig. 5c is somewhat higher than the minimum at $x=1$; in fact, the curve follows quite closely that of Eq. (15) (not shown), except it is lying slightly above it. We note that the lower left of Fig. 4 gives a spanwise circulation based on Eq. (14), which represents rather closely the elliptic distribution except near the tip. The departure from the elliptic load near the tip accounts for the slight increase above $1/2\pi$ at $x=1$.‡‡ The minimum of $T(x)$ under fixed F_x^2 is

$$T_{\min}(x) = \left(\frac{1}{4\pi}\right)F_x^2 \ell n\left(\frac{2}{a}\right) \qquad (16)$$

††Elliptic spanwise distribution of the circulation is an optimum under a fixed span; however, an optimum distribution other than elliptic results, if, for example, a fixed bending moment at mid-span is specified (cf. Jones, Ref. 20).

‡‡The minimum $E(x)$ under fixed $F(x)$ requires an infinite $[\![\varphi_x]\!]$ at the leading edge and, therefore, cannot be fully realized under shock-free entry.

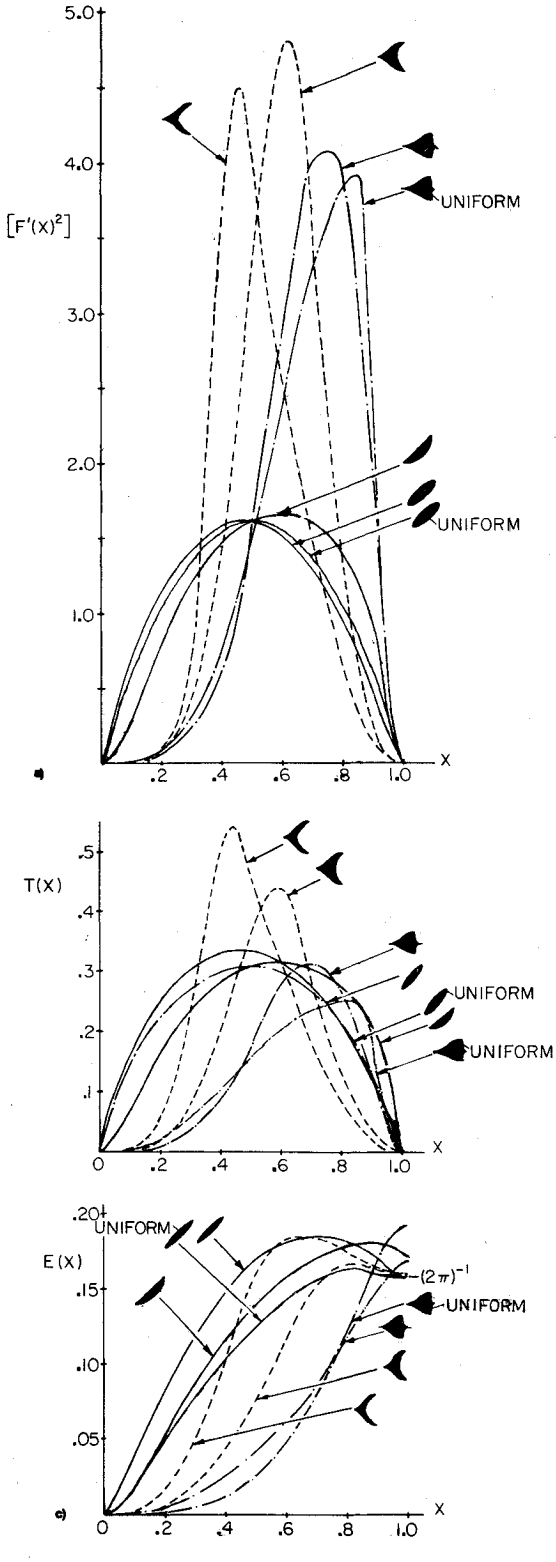

Fig. 5 Distributions F_x^2, $T(x)$, and $E(x)$ contributing to equivalent body area.

which is about 10-15% below the dash-dot curve in Fig. 5b.

To illustrate the degree to which the assumed form of $[\![\varphi]\!]$ or $[\![\varphi_x]\!]$ may affect $S_e(x)$, we also include in Figs. 5a-c the corresponding results for a uniform load, i.e., $[\![\varphi_x]\!]$ = constant, where the constant is determined by $F(1)=1$. The results presented in dash-dot line is labelled with the word "uniform." Obviously, the differences resulting from altering from the load of Eq. (14) to that of Eq. (16) is quite limited.

Symmetric Swept Wings

The two swept-wing planforms shown in Fig. 3b and the corresponding distributions of F_x^2, E, and T are computed with a leading-edge contour which is sinusoidal in $\frac{1}{2}\pi x^{1.575}$, and a trailing-edge contour which is hyperbolic. The leading-edge turns out to be reasonably close to that of the Concorde in Fig. 3a. A load distribution generally may be assumed as $x_{l.e.}<x<x_{t.e.}$,

$$[\![\varphi_x]\!] = a_o(x)\,|x-x_{l.e.}(y)|^{1/2}[x_{t.e.}(y)-x]Q(x;y) \qquad (17)$$

where $x=x_{l.e.}(y)$ and $x=y_{t.e.}(y)$ are the equations for the leading-edge and trailing-edge contours, respectively, and $Q(x;y)$ is a polynomial with the coefficients being functions of y. As noted before, the F_x^2, E, and T of interest do not appear to be too sensitive to changes in the distribution $[\![\varphi_x]\!]$ over a fixed planform. A more critical dependence is to be found in the changes in the planform contour. It suffices, therefore, for the present purpose to set, in Eq. (17),

$$Q(x;y)=1 \qquad (18)$$

The function $a_o(y)$ in Eq. (17) is then determined by the elliptic spanwise load at the trailing edge

$$[\![\varphi]\!]_{t.e.}=\left(\frac{2}{\pi}\right)\sqrt{1-y^2} \qquad (19)$$

consistent with $F(1)=1$.§§

The two sets of results corresponding to the two swept wings are given in Fig. 5a-c as dotted curves. Compared to the Concorde (dash-dot curve), the symmetric swept wings have higher peaks in $(F_x)^2$ and $T(x)$; their gradients are accentuated, and their peaks shifted further upstream, as the aspect ratio increases. This trend is not unexpected, since, with $F(1)=1$ and the span load $[\![\varphi]\!]_{t.e.}$ fixed, $[\![\varphi_x]\!]$ increases as the local chord decreases; a higher aspect ratio should, therefore, bring about higher F_x^2 and higher $T(x)$ [cf. Eq. (10)]. The higher values of F_x^2 compared to the Concorde are a direct consequence of the lifting area reduction on the downstream side. For the $E(x)$, the changeover from the Concorde to symmetric swept-wing planforms by cutting out portions of trailing edge increases greatly the $E(x)$ over the central part of the x-range, causing overshoots above its terminal value $1/2\pi$, which is quite pronounced with the higher aspect ratio.

The values of E and T are computed from the formulas given below Eq. (10) as iterated integrals in y and y_1. For the x-station intersecting the trailing edges, each single integration in y or s contain three segments of distinctly different analytical descriptions of $[\![\varphi_x]\!]$ and $[\![\varphi]\!]$. The integration algorithm treats the logarithmic singularity in both $E(x)$ and $T(x)$. Special treatment in the integration method for square root singularity at the leading edge is unnecessary for the symmetric swept wing, since the resulting errors in F_x^2, E, and T are of the order $(\Delta y)^{3/2}$. The smallest number of divisions used in discretizing y and y_1 for applying the trapezoidal rule is 40.

Oblique Wings

Two variations in planform are considered for the oblique wings (cf. Fig. 3c). One version has an elliptic contour with the major to the minor axes in the proportion 10:1 when $\lambda=b/c_o=1$. The second planform has a straight leading edge and a trailing edge described by a polynomial in y^2, giving a pointed tip; the ratio of the span to the normal chord when $\lambda=1$ is again 10:1. For the oblique elliptic wing, two load distributions are studied. One employs a variable load, the same as Eq. (17) with $Q=1$, and with an elliptic spanwise circulation distribution Eq. (19). The other is a uniform load,

§§Note that $[\![\varphi]\!] = [\![\varphi]\!]_{t.e.}$ for the same y over the trailing-vortex sheet.

with the constant fixed by $F(1)=1$. For the second planform with a straight leading edge, only the uniform load is considered.

The integration methods similar to those used for the symmetric swept wings are employed, but care must be exercised in defining the trailing edge and leading edge for the yawed ellipse, which do not correspond exactly to the elliptic contours downstream and upstream of the major axis. Distinct subranges of integrations must be considered accordingly. The error in the $E(x)$ integration is considerably greater for the elliptic wing, being of the order of the square root of the (smallest) step size. This results from the inverse square-root singularity in $[\![\varphi_y]\!]$ along the entire side edge of the trailing-vortex sheet affecting most parts of the oblique wing. The resulting accuracy in $E(x)$ for the elliptic wing is nevertheless adequate; a test at $x=1$ for different Δy or Δy_l corresponding to 10 to 130 divisions, shows a departure from the exact value $1/2\pi$ no greater than 1.1%.

The computed results for the three oblique wings are presented in Figs. 5a-c as full curves. Note that the distributions F_xE, and T are given over the range $0<x<1$ based on the reference scale c_0. Comparing the three oblique wing results with those of the Concored and the symmetric swept wings (cf. Fig. 5a-c), the oblique wing results are considerably smoother (less peaked) with greatly reduced maxima in $(F_x)^2$ (by a factor of three). This difference results from the fact that the front parts of the symmetric arrow-headed wings are more lightly loaded than is the forward wing tip of the oblique design. On the other hand, the differences among the three cases of oblique wings are not very pronounced.

V. Application to Transport Design Study

In order to assess the importance of the lift effects on the outer flow for transport designs, we shall study below the distributions of S_e and $(\sigma_l F_x)^2$ for a specific set of parameters σ^2, Γ., and ϵ corresponding to a realistic design.

A. Change of the Axial Reference Length

As pointed out earlier, extensive calculations of the lift effects made in Sec. IV for the wing alone may be applied to a complete airplane after a change of variables (as well as the definitions of the parameters) to be shown below. It is stipulated that the lift distributions is little affected by the introduction of the wing thickness and the fuselage.

It is essential to distinguish the axial reference length l (for the equivalence rule application) from the overall chord of the lifting surface c_o. Unless lift dominates in the outer flow, i.e. $\sigma_\cdot >>1$, we may take l to be the length characterizing the thickness distribution, which is the overall length of the complete airplane in most cases.

With the definition $\tilde{x}\equiv x^*/l$ remaining unchanged (cf. Sec. III), the variable x appearing in $F'(x)$, $T(x)$, and $E(x)$ of Sec. IV must now refer to

$$x\equiv (x^*-x_o^*)/c_o \tag{20}$$

where the asterisk refers to physical quantities and x_o^* is the physical x-coordinate of the wing apex. Since $\mathrm{d}/\mathrm{d}\tilde{x}=(l/c_o)\,\mathrm{d}/\mathrm{d}x$, the functions $F'(x)$, $E(x)$, and $T(x)$ for the wing alone are related to their counterparts for the complete airplane as follows:

$$\left(\frac{\mathrm{d}F}{\mathrm{d}\tilde{x}}\right)^2=\left(\frac{l}{c_o}\right)^2\left(\frac{\mathrm{d}F}{\mathrm{d}x}\right)^2 \tag{21a}$$

$$\tilde{T}(\tilde{x}) =\left(\frac{l}{c_o}\right)^2 T(x) \tag{21b}$$

$$\tilde{E}(\tilde{x}) =E(x) \tag{21c}$$

The last two terms of Eq. (21) follow from their definitions given below Eq. (10). Thus, the lift contribution to the equivalent-body cross-sectional area can be computed in terms of $F'(x)$, $T(x)$, and $E(x)$ of Sec. IV as

$$S_e(\tilde{x})-S_c(\tilde{x}) =\sigma^2\left(\frac{l}{c_o}\right)^2[(\|\pi)^{-1}(1+2^{-1}|\ell n\epsilon|^{-1})F_x^2 +2^{-1}|\ell n\epsilon|^{-1}T(x)]+8^{-1}\sigma^2\Gamma_\cdot E(x) \tag{22}$$

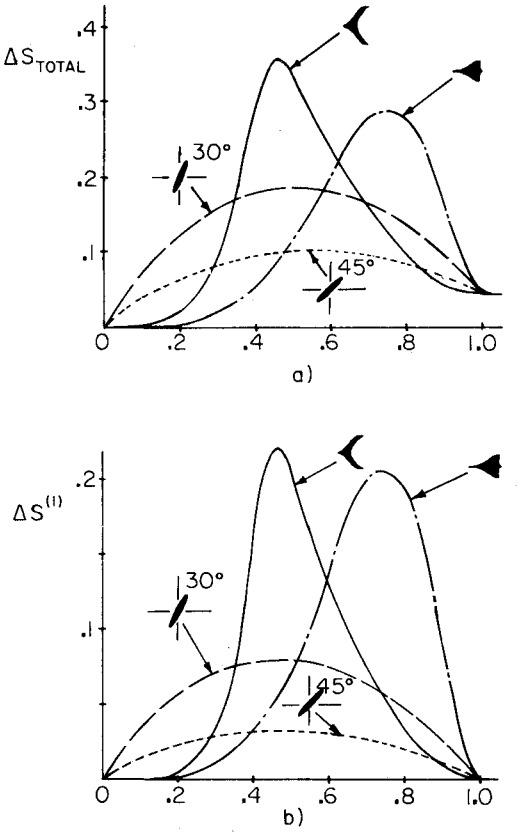

Fig. 6 Lift contribution to equivalent-body cross-section area, $S_e(x)$, and to distribution $\Delta S^{(l)}$ calculated for three representative lifting surfaces.

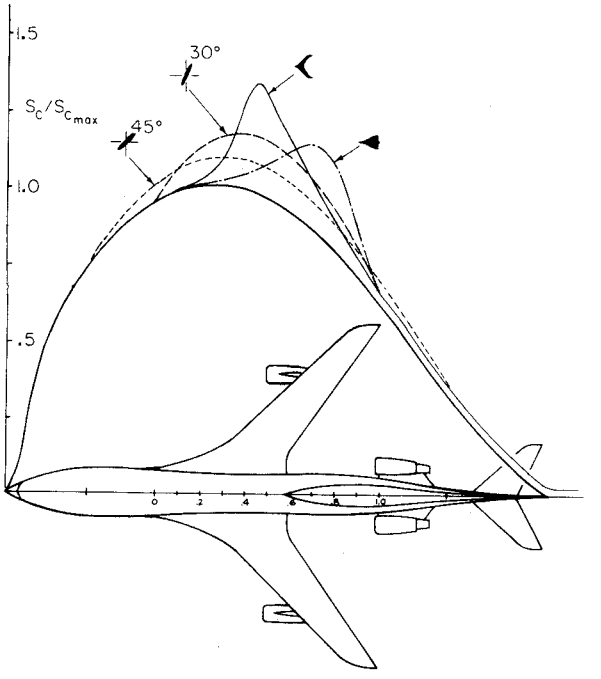

Fig. 7 Equivalent-body cross-sectional area of Mach 0.98 design with four alternative lifting-surface arrangements.

For a *given* lifting surface, solutions to the velocity and pressure are independent of the choice of reference length scales l and b, but the size the dimensionless variables may be affected by their choice. Nevertheless, the lift contribution to $S_e(x)$ is *not* so strongly dependent on the choice. A decrease in σ_*^2 due to doubling l, for example, is compensated almost exactly by an increase in F_x^2, $T(x)$, and Γ_*; the only change in S_e in this instance is in the factor $|\ell n \epsilon|$ weakly dependent on l and b.¶¶ For the different lifting surfaces to be considered below, where b and l or c_o are fixed, this (slight) ambiguity on the reference lengths should not arise, and the comparison (among different cases) is, therefore, unambiguous.

B. Lift Contributions to S_e: Mach .98 Design

The study will be confined to Goodmanson's design[15] cited earlier in Sec.IIID. The specifications needed for the determination of ϵ, σ_*^2, and Γ_*, or $\sigma_*^2\Gamma_*$ for this case are: $M_\infty = 0.98$, Gross Wt. = 287,300 lb, altitude = 39,000 ft ($p_\infty \simeq 411$ lb/ft^2), $b \simeq 60$ ft, $c_o \simeq 80$ ft, $l = 171$ ft (body length), and $S'_{\max} = 270$ ft^2. This yields

$$\sigma_*^2 (l/c_o)^2 = (\gamma+1) M_\infty^2 |\ell n \epsilon| (\text{Lift}/\gamma p_\infty M_\infty^2 c_o)^2 (S'_{\max})^{-1} = 1.072,$$
$$8^{-1}\sigma_*^2\Gamma_* = (\gamma+1)^{-1} |\ell n \epsilon|^{-1} (l/b)^2 \sigma_*^2 = 0.2671, \qquad (23)$$
$$\epsilon = |(\gamma+1) M_\infty^2 \tau (b/l)^3|^{1/2} = 0.0512$$

With these values, the lift contribution to $S_e(x)$ reads

$$S_e - S_c = (0.3136) F_x^2/2\pi + (0.1803) T(x) + (0.2671) E(x) \qquad (24)$$

Note that the design specifications, under which Eq. (24) is applicable, have fixed the overall chord c_o, the half-span b, and the length l, leaving the planform unspecified. Note also from the above that the total lift is equated to the take-off weight (which were the only weight data available to the author). The lift effect in question may be considerably smaller at the end of the cruise.

Since the exact planform and load distribution data in Goodmanson's design[15] are not available, the results obtained in Sec. IV B for the symmetric swept planform A (Fig. 3b) are taken to be representative. We note that planform A (applied to the specified b and c_o) gives a leading-edge sweep angle of 43.5° at mid-span compared to 42.5° inferred from Goodmanson's design.[15] Although, the aspect ratio of the planform A appears to be higher than Goodmanson's (cf. sketches in Figs. 3 and 7), the study in Sec. IVB on the symmetric swept wings (cf. Figs. 5a-c) suggest that their limited difference in aspect ratio cannot produce significant changes in F_x^2, T, and E. The result of application of Eq. (24) to planform A is presented in Fig. 6(a) in the thin full line. The first term on the right-hand side of Eq. (24) is essentially $(\sigma_l F_x)^2$ and is the largest among the three terms. This quantity, denoted by $\Delta S^{(1)}$, is given in Fig. 6b. In the present case, the last term of Eq. (24) involving $E(x)$ turns out to be relatively small; nowwhere does it exceed 5% of the maximum S_c'. The total equivalent-body cross-sectional area for this symmetric swept-wing design is plotted (in the full thin line) in Fig. 7, where the very smooth geometrical cross-sectional area $S_c(x)$ (in the full thick line) is taken from the original Goodmanson design.[15]

Planform Changes Affecting S_e and $(\sigma_l F_x)^2$

As a study assessing the importance of the lift effect, it is essential to explore the changes in S_e and $(\sigma_l F_x)^2$ which can be effected through changes in wing planform for an otherwise identical design. We consider for this purpose two alternative planforms: the Concorde (cf. Fig. 3a) and the elliptic oblique (cf. Fig. 3c) analyzed previously in Sec. IV.

The switch from one planform to another must entail some rearrangements for the wing-root location accompanying the center of gravity and structural changes, as well as an increase in the wing area in switching over to the Concorde (if the same b and c_o are maintained). These, together with the achievement of a smooth $S_c(x)$ distribution, are assumed to be feasible within the state of the art of airplane design to date. Our chief concern is to examine and demonstrate the degree to which wing morphology affects the equivalent-body area and other distributions in some concrete specific cases.

As noted earlier, the formula for the lift contribution to $S_e(x)$, Eq. (24), is applicable to designs with alternative planforms but the *same* half span and overall chord. With $(F_x)^2$, $T(x)$, and $E(x)$ provided in Figs. 5a-c, $(S_e - S_c)$ for the Concorde and the elliptic oblique wings are computed and presented in Fig. 6a as dash-dot and dashed curves, respectively. Only cases with a variable load are considered. The accompanying $(\sigma_l F_x)^2$ distributions are included in Fig. 6b. Because c_o is fixed, the oblique wing corresponding to the dashed curves in Fig. 6 must sweep at a smaller angle than the symmetric swept wing does.

Comparing the three alternatives with the same b and c_o, the symmetric wing (in thin full lines) gives the highest and most peaked additions to the cross-sectional area and the $(\sigma_l F_x)^2$ distribution. The oblique alternative (in dashes) yields the least and smoothest addition to S_e and to $(\sigma_l F_x)^2$.

These results on $(S_e - S_c)$ superimposed to the $S_e(x)$ of the original design are shown in Fig. 7 as dash-dot and dashed curves. Thus, it appears that the problem posed by the lift effect may be alleviated through the alternative of adopting an oblique or Concorde type planform. The excessively large wing area of the Concorde may be reduced further by taking a smaller span, which should also reduce the dominant term of $(S_e - S_c)$. Similar, and perhaps more significant, is the greater reduction of the nonlinear lift effect through a more realistic oblique wing design. We note that the smaller sweep angle for the oblique wing called for by the fixed c_o would necessitate the use of an airfoil section thinner than, and substantially different from, that employed in the original swept-wing design. To exploit the advantage of the oblique wing design fully (Jones,[20,21] Jones and Nisbet[22]), one must remove the restriction on c_o so that the oblique and symmetric swept wings may have the same sweep angle and, thus the same component Mach number. This should significantly reduce σ_*^2, hence, the contributions of F_x^2 and $T(x)$ to $S_e(x)$; however, the first two coefficients in Eq. (24) have to be revised in this case.

Asymmetrical Design Reconsidered

We shall now revise the value of σ_*^2 for the oblique wing to allow for an increase in c_o so that the yaw angle may reach 45°. The new value of c_o is taken to be 1.6 times the original value (which is 7% larger than 120 ft, to allow for tip fairing). Thus, for the asymmetrical design with 45° yaw at Mach 0.98, the coefficients of the first two terms on the right-hand side of Eq. (24) are to be changed according to Eq. (21) to the smaller values 0.1225 and 0.0704, respectively. Recalling the significant difference in F_x^2 between symmetric and asymmetric swept wings (Fig. 5a), the design under consideration should reduce significantly the lift contribution to $S_e(x)$ and $(\sigma_l F_x)^2$. This drastic reduction is substantiated by calculations based on the revised ΔS and $\Delta S^{(1)}$, presented in Figs. 6 and 7 as short-dash curves. We observe that the maximum equivalent area increase due to lift for the oblique design is reduced to one quarter of that for the symmetric wing of comparable sweeps, with an almost eight-fold reduction in the equivalent source strength, dS_e/dx. In contrast to the peaked distribution for the symmetric design (with a conspicuous crest), the area increase for the asymmetric design differs little from the geometrical area $S_e'(x)$.

¶¶There is a corresponding change in $\sigma_l(\log \eta)^2$ in Eq. (7), which cancels out exactly the change in $|\ell n \epsilon|$ of $S_e(x)$, so that the solution is independent of the reference scale l.

VI. Concluding Remarks

Lift correction to the area rule represents an essential aspect in the analysis of modern aircraft designed to operate in the transonic range. In this paper, we have summarized the theory of the transonic equivalence rule involving lift, discussed its requirements, and studied the lift effects for a number of wing planforms and load distributions. Of the four parameters given in Eq. (3), the most important is σ^2 which controls the lift correction in question. There are two functions essential in determining the strength of the line source and line doublet in the equivalence rule, namely, $S_e(x)$ and F or F_x^2. Calculations for the lift contributions to $S_e(x)$ and F_x^2 have been made from three families of planforms (Concorde, symmetric swept, and oblique). The results are applied to a study of the lift corrections for a Mach 0.98 transport, with alternative wing designs.

The maximum of $S_e(x)$ involving lift is found to be 35% above its zero-lift value, which rises abruptly, giving a rather peaked apperance in the $S_e(x)$ distribution. The equivalence-body area increase is the least and smoothest for the (oblique) asymmetrical arrangement. By changing over from a symmetrical to an asymmetrical design, while maintaining the same component Mach number, the maximum of the S_e increase due to lift can be reduced by a factor of four, with a nearly eight-fold reduction in the correction to the equivalent source strength, dS_e/dx. For a symmetric planform, the adverse lift corrections may, nevertheless, be reduced by increasing the leading-edge sweep angle which should effectively suppress σ^2. This possibility should be more closely examined in future design analyses. Since quantitative differences in results are expected to arise from differences in planform or loading, some caution must be exercised against oversimplification in the wing shape and lift representation.

Acknowledgments

The study was supported by the Office of Naval Research Fluid Dynamics Program, Contract Number N00014-75-C-0520. The work was presented at the ONR Transonic Flow Conference held at Univ. of Calif., Los Angeles, March 18-19, 1976. Valuable assistance has been provided by B. A. Toresch, S. Y. Meng, and L. Murillo. Stimulating discussions with M. Cooper are much appreciated.

References

[1]Whitcomb, R. T., "A Study of the Zero-Lift Drag Rise Characteristics of Wing Body Combination Near the Speed of Sound," NACA RM-L52H08, 1952, (superseded by TR 1273, 1956).

[2]Oswatitsch, K. and Keune, F., "Nichtangestellte Kortper kleiner Spannwite in Unter-und Uberschallströmung," *Proceedings of the Eighth International Congress Theoretical and Applied Mechanics*, Istanbul, 1952.

[3]Oswatitsch, K. and Keune, F., "Ein Äquivalenz-Satz für nichtangestellte Flügel kleiner Spannweite in schallnaher Strömung," *Zeitschrift für Flugwissenschaft*, Vol. 3, No. 2, 1954, pp. 29-46.

[4]Cheng, H. K. and Hafez, M. M., "Equivalence Rule and Transonic Flows Involving Lift," University of Southern California, School of Engineering, Department of Aerospace Engineering Report USCAE 124, April 1973, see also Cheng., H. K. and Hafez, M. M., "Equivalence Rule and Transonic Flow Theory Involving Lift," *AIAA Journal*, Vol. 11, Aug. 1973, pp. 1210-1212.

[5]Cheng, H. K. and Hafez, M. M., "Transonic Equivalence Rule: A Nonlinear Problem Involving Lift," *Journal of Fluid Mechanics*, Vol. 72, 1975, pp. 161-188.

[6]Jones, R. T., "Properties of Low-Aspect Ratio Pointed Wings at Speed Below and Above the Speed of Sound," NACA Report 835, 1946.

[7]Ward, G. N., "Supersonic Flow Part Slender Bodies," *Quarterly Journal of Mechanics and Applied Mathematics*, Vol. 2, Pt. 1, 1949, pp. 75-97.

[8]Cole, J. D. and Messiter, A., "Expansion Procedures and Similarity Laws for Transonic Flow, Part I. Slender Bodies at Zero Incidence," *Zeitschrift für Angewandte Mathematik und Physik*, Vol. 8, pp. 1-25.

[9]Ashley, H. and Landahl, M., *Aerodynamics of Wings and Bodies*, Addison-Wesley, Reading, Mass., 1965.

[10]Spreiter, J. R. and Stahara, S. S., "Aerodynamics of Slender Bodies and Wing-Body Combinations at M = 1," *AIAA Journal*, Vol. 9, Sept. 1971, pp. 1784-1791.

[11]Hayes, W. D., "Pseudotransonic Similitude and First-Order Wave Structure," *Journal of Aeronautical Science*, Vol. 21, Nov. 1954, pp. 721-730.

[12]Cheng, H. K. and Hafez, M. M., "Three-Dimensional Structure and Equivalence Rule of Transonic Flows," *AIAA Journal*, Vol. 10, Aug. 1972, pp. 1115-1117.

[13]Barnwell, R. W., "Transonic Flow about Lifting Configurations," *AIAA Journal*, Vol. 11, May 1973, pp. 764-766.

[14]Barnwell, R. W., "Analysis of Trasonic Flow about Lifting Wing-Body Configurations," TR R-440, June 1975.

[15]Goodmanson, L. T., "Transonic Transport," *Aeronautics & Astronautics*, Nov. 1971, pp. 46-57.

[16]Goodmanson, L. T. and Gratzer, L. B., "Recent Advances in Aerodynamics for Transport Aircraft," *Aeronautics & Astronautics*, Dec. 1973, pp. 30-45.

[17]Whitcomb, R. T., et al., "Supercritical Wing Technology-A Progress Report on Flight Evaluations," NASA Flight Research Center, Edwards, Calif., Memo, Feb. 1972.

[18]Bauer, F., Garabedian, P. R., Korn, D. G., and Jameson, A., *Supercritical Wing Section*, Springer-Verlag, Berlin, 1973.

[19]Nieuland, G. Y. and Spee, B. M., "Transonic Airfoils: Recent Developments in Theory, Experiment and Design," *Annual Review of Fluid Mechanics*, Vol. 5, 1973, pp. 119-150.

[20]Jones, R. T., "The Spanwise Distribution of Lift for Minimum Induced Drag of Wings Having a Given Lift and a Given Bending Moment," NACA TN 2249, 1950.

[21]Jones, R. T., "Reduction of Wave Drag by Antisymmetric Arrangement of Wings and Bodies," *AIAA Journal*, Vol. 10, Feb. 1972, pp. 171-176.

[22]Jones, R. T. and Nisebet, J. W., "Transonic Transport Wings-Oblique or Swept?," *Astronautics & Aeronautics*, Jan. 1974, pp.40-47.